Inflation of the edge of chaos in a simple model of gene interaction networks

Dejan Stokić,[1] Rudolf Hanel,[1] and Stefan Thurner[1,2,*]
[1]*Complex Systems Research Group, HNO, Medical University of Vienna, Währinger Gürtel 18-20, A-1090 Vienna, Austria*
[2]*Santa Fe Institute, 1399 Hyde Park Road, Santa Fe, New Mexico 87501, USA*
(Received 29 November 2007; revised manuscript received 1 April 2008; published 18 June 2008)

We study a set of linearized catalytic reactions to model gene and protein interactions. The model is based on experimentally motivated interaction network topologies and is designed to capture some key properties of gene expression statistics. We impose a nonlinearity to the system by enforcing a boundary condition which guarantees non-negative concentrations of chemical substances. System stability is quantified by maximum Lyapunov exponents. We find that the non-negativity constraint leads to a drastic inflation of those regions in parameter space where the Lyapunov exponent exactly vanishes. Within the model this finding can be fully explained as a result of a symmetry breaking mechanism induced by the positivity constraint. The robustness of this finding with respect to network topologies and the role of intrinsic molecular and external noise is discussed. We argue that systems with inflated "edges of chaos" could be much more easily favored by natural selection than systems where the Lyapunov exponent vanishes only on a parameter set of measure zero.

DOI: 10.1103/PhysRevE.77.061917 PACS number(s): 87.16.Yc, 64.60.Ht, 82.39.Rt

I. INTRODUCTION

Most complex systems, living systems in particular, are characterized by remarkable degrees of stability and at the same time by a tremendous potential of flexibility and adaptability. This has led some authors to define complex and living systems as living at the "edge of chaos," [1–4] meaning—in a somewhat picturesque way—that it takes only tiny changes in the system to move it from a stable and regular mode into a chaotic phase where large portions of phase space can get sampled. The concept is that systems at the edge of chaos are especially well-suited for adaptation and information processing in the sense that adaptability is associated with the possibility of finding adequate new states in possibly changed environments at very fast rates. It has been argued that living systems at the edge of chaos would get favored by natural selection, and that life has evolved toward such a special region in parameter space [2]. In many dynamical systems the edge of chaos is a very special set of points in parameter space, often of measure zero, characterized by the system's maximal Lyapunov exponent (MLE) λ passing through zero. It is not clear how systems can get regulated toward (or have evolved toward) such a limited set of critical points, even though some interesting ideas have been proposed in this direction [5]. Even in the simplest maps like the logistic map, the dynamics exactly at these special points can become highly nontrivial [6].

It is evident that living systems have evolved toward stable systems in stationary disequilibrium. Various authors argue that a key principle of living systems is their ability to replicate [7]; corresponding rate equations for molecular replicators have been proposed for a long time, beginning with Ref. [8]. As such, basic molecular reactions in living systems (e.g., protein production or degradation) have to be autocatalytic. If autocatalytic reactions are not balanced by degradation and/or thermostatic net-flow of substance to and from the system (like in a flow reactor), concentrations of molecular products will diverge in the replicator. A stationary state can be established when production and decay (flow) rates of intercellular molecules effectively balance each other [9,10]. In this sense stability (stationarity) provides a natural selection criterion. Cells can turn from a stable genetic dynamics toward an unstable one, for example, through viral infections. Viral genetic material can cause the cell to produce a viral protein at rates that eventually cause cell death. It is intuitively clear that all mutations or variations of a cell that turn a stable system into an unstable one eventually cause the system to collapse thus favoring variations with stable dynamics in an evolutionary sense.

Catalytic reactions can be simply described by reaction networks which quantify production and degradation rates. Given current developments in genomics and proteomics technology some facts about these networks become known. By now there is some evidence that these (directed) networks show scale-free (SF) topological organization [11,12]. On the basis of a given molecular reaction topology [13] several gene network models have been proposed [14–16]. In principle two different approaches have been pursued: discrete approaches, using Boolean networks [17], and continuous approaches, using ordinary or stochastic differential equations [18–21]. Combinations of both have also been reported [22,23]. It is remarkable that disordered recurrent networks, whether modeled with Boolean, or S-state discrete recurrent networks with piecewise linear equations [17] or mean-field models of chemical master equations [24], all seem to share three distinguished modes of operation: (i) a stable, (ii) a critical, and (iii) a chaotic supercritical region. There is evidence that this property could be generic or even *universal*. It is important to ask about the minimum complexity of a model showing these properties, in particular whether a linear ordinary differential equation (i.e., linear catalytic equations) would be sufficient [17].

Recently the importance of noise in molecular reaction networks has been stressed and its relevance has been experimentally demonstrated [25–27]. For example, the level of noise can determine whether cells in Drosophila become epi-

*thurner@univie.ac.at

dermal or neural cells [28]. Further it was shown that low reproduction rates of DNA and important regulatory molecules forbid one to neglect stochastic effects [29]. Intrinsic noise, microscopic events within the cell, and extrinsic noise, such as cell to cell variations, are now experimentally distinguishable [30], and stochastic differential equation models have been proposed for regulatory transcription networks, e.g., Ref. [31].

In this work we study a simple linear, noise driven dissipative model for catalytic molecular reactions governing the concentration levels of sets of molecular species. The nonlinearity is introduced through a natural restriction on the domain of the process: concentrations are always nonnegative. We demonstrate that this nonlinearity changes the "edge of chaos" from a point where $\lambda=0$, to extended regions of vanishing MLE. This inflation of the "edge of chaos" in parameter-space is crucial for understanding how systems displaying stable and nontrivial dynamics at the same time can emerge by pure chance. The model offers a full explanation for this inflation of the "edge of chaos."

II. MODEL

We assume that gene-to-gene interactions can be modeled as chemical reactions between proteins, mRNA, and other nucleic material. Chemical rate equations considered in this context are usually nonlinear such as the quadratic differential Michaelis-Menten equations [32], expressions for enzyme-kinetics, or more general replicator dynamics, e.g., Ref. [33]. For the case of abundant substrate concentrations these catalytic network equations have been linearized, e.g., in Refs. [34,35]. In this form linear models have been used extensively for reverse engineering of gene networks, see, e.g., Ref. [36].

Let us denote the concentrations of proteins α at time t by a vector $p_\alpha(t)$, and those of RNA molecules i by $x_i(t)$. Collecting both types of concentrations into a N-dimensional vector $y=(p,x)$ dynamics will be given by an appropriate nonlinear equation, $\dot{y}_i=F_i(y)$. Boundedness of the system implies the existence of a limit cycle or a fixed point. We assume the existence of at least one fixed point y^0 and linearize the system around it. Since (m)RNA usually directly codes proteins it is natural to assume a linear dependence of a perturbation of RNA concentration, $\delta x=x-x^0$, and the associated protein perturbation vector, $\delta p_\alpha=\Sigma_i C_{\alpha i}\delta x_i$, where $C_{\alpha i}$ encodes the linear transcription of (m)RNA into a protein. Near the fixed point the system becomes

$$\frac{d}{dt}\delta x_i=\sum_j\left(\frac{\partial}{\partial x_j}F_i(y^0)+\sum_\alpha\frac{\partial}{\partial p_\alpha}F_i(y^0)C_{\alpha j}\right)\delta x_j, \qquad (1)$$

now in terms of RNA concentrations only. By identifying the terms in the bracket with an effective gene-to-gene interaction matrix, A^0, and noting that $\delta\dot{x}=\dot{x}$, we arrive at the simplest linear model to capture all possible gene-to-gene interactions,

$$\frac{d}{dt}x_i=\sum_j A^0_{ij}(x_j-x^0_j). \qquad (2)$$

Even though linear models of this kind are clearly an oversimplification of reality they have frequently been used recently [36,15,37]. Assume that interaction rates are not perfect constants but fluctuate according to $A^0_{ij}(t)=A_{ij}+\xi_{ij}(t)$, for example, through thermal noise or fluctuations of catalyst (protein) levels. For simplicity let the ξ_{ij} be independent identically distributed (iid) processes with zero mean. Replacing A^0 by A we get

$$\frac{d}{dt}x_i=\sum_j A_{ij}\delta x_j+\xi_{ii}(t)\delta x_i+\sum_{j\neq i}\xi_{ij}(t)\delta x_j. \qquad (3)$$

Regardless of the distribution of ξ_{ij}, and assuming that x will converge to a reasonably stationary distribution, according to the central limit theorem, the sum of the right-hand side, $\eta_i\equiv\Sigma_{j\neq i}\xi_{ij}(t)\delta x_j$, yields a random number from a Gaussian distribution, which we denote by $\eta_i\in N(0,\sigma)$. This produces additive noise terms. For simplicity we assume ξ_{ii} also to be Gaussian, i.e., (with a little abuse of notation) $\xi_{ii}\equiv\xi_i\in N(0,\bar{\sigma})$, with the same variance $\bar{\sigma}$, $\forall i$. This defines the multiplicative noise terms.

A note on the fixed point x^0. It has a natural interpretation as the characteristic RNA concentrations around which actual levels oscillate during a cell cycle. x^0 can be measured experimentally to a certain extent. In Fig. 1(a) we show experimental mRNA expression levels of the yeast genome (*S.cerevisae*) over two cell cycles at 17 time points taken at 10 min intervals [38]. In this view x^0 could be defined as the time-average over cell cycles, $x^0_i=\langle x_i(t)\rangle_t$. These experimental values for the components of x^0 can be fed directly into the model. However, note that from a theoretical point of view setting $x^0=0$ also is a perfectly legitimate choice. In the following the components of the fixed point $x^0_i>0$ are taken from the experimental yeast distribution [38,39], shown in Fig. 1(b). We verified that our results are largely independent of the particular choice of x^0, in particular we have performed all computations also with uniform and Gaussian random vectors; we will explicitly demonstrate the case for $x^0=0$ below. The complete model thus reads

$$\frac{d}{dt}x_i=\sum_j A^0_{ij}(x_j-x^0_j)+\xi_i(t)(x_i-x^0_i)+\eta_i, \qquad (4)$$

with $\xi_i\in N(0,\bar{\sigma})$ and $\eta_i\in N(0,\sigma)$, the multiplicative and additive noise components, respectively. Multiplicative and additive noise have been interpreted as intrinsic and extrinsic noise as used, e.g., in Ref. [30].

To interpret x as concentrations we have to introduce the constraint

$$x_i(t)\geq 0 \quad \forall\, i,t, \qquad (5)$$

which means that regardless of $\dot{x}_i$ in Eq. (4), $x_i(t)$ can never become negative.

A. Interaction matrix

Before solving the system we have to specify the interaction network, i.e., the matrix elements (chemical rates) of A.

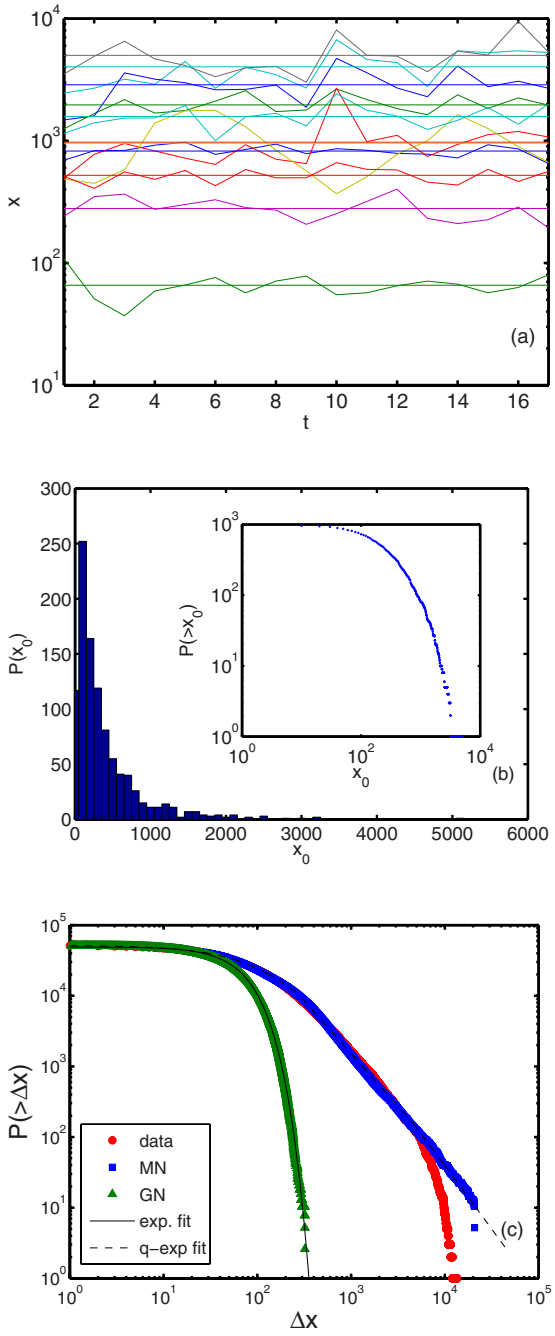

FIG. 1. (Color online) (a) Ten randomly picked gene-expression trajectories of yeast (*S. cerevisiae*) over two cell cycles [38], $N=6220$. Fixed point values x^0 are defined as the time-averages of gene expression levels (horizontal lines). (b) Distribution of stationary state values x^0; inset: cumulative distribution. (c) Cumulative distribution of gene expressions increments for the same data (circles) for the numerical simulation of the evolution of gene expression data with only multiplicative noise only (boxes) and pure additive Gaussian noise (triangles). Data is well-fitted by a q Gaussian (broken line).

It is obvious that the network is directed and weighted. Diagonal elements $A_{ii}<0$ are decay rates, off-diagonal rates A_{ij} can be positive or negative corresponding to activation or inhibition. Not all products can interact with each other, i.e., a large number of matrix elements will be zero; most rates are presently not available from experiments. We thus model A as a sparse random matrix in the following way. Using terminology from network theory the "degree" k_i of product i is defined as the number of products that can be regulated by product i. The class of interaction networks can now be specified by the "degree distribution." There is evidence that protein networks [12] and metabolic networks [13] are scale-free (SF) networks $p(k)\sim k^{-\gamma}$, characterized by a degree distribution with average degree $\langle k\rangle>4$, and an exponent $\gamma\sim 2.2$. Below we generate SF networks and contrast them to random networks, i.e., Erdös-Renyi graphs (ER) [40] with the same average degree. If the number of nonzero rates in A is denoted by L, the average connectivity is $\langle k\rangle=L/N$. Once it is decided which products interact with each other, i.e., $A_{ij}\neq 0$, the actual rates have to be fixed. We assume these being Gaussian, $A_{ij}\in N(0,\sigma_A)$. This is supported experimentally, e.g., by Ref. [37], where a least-squares fit of synthetic gene network models to real data indicates that the normal distribution of interaction weights provides the best results. In the following we take the (negative) decay rates A_{ii} constant and identical for all i.

Note that σ_A and the decay rates A_{ii} are not independent variables but that the quotient

$$D \equiv -\frac{A_{ii}}{\sigma_A} \tag{6}$$

governs the characteristic behavior of the dynamics. σ_A can be absorbed into a redefinition of the time scale and the noise amplitudes. Thus without loss of generality we set $\sigma_A=1$ for all simulations. For later use we call a node i, *on*, when its concentration value $x_i(t)>0$ and *off* otherwise, and assign N_{on} and N_{off} to the number of *on* and *off* nodes, respectively, i.e., $N=N_{on}+N_{off}$.

B. Stability

If we ignore for a moment the positivity condition, Eq. (5), and the stochastic terms in Eq. (4), the stability of the system is dominated by the largest real part of the eigenvalues of the interaction matrix A. If there are no non-negative real parts of the eigenvalues, the system will be asymptotically stable. If the distribution of off-diagonal elements in A is normal [37] with variance σ_A^2, the eigenvalue spectrum is—according to a result from random matrix theory—a circle in the complex plane (Girko's circular law) [42]. For a fully connected matrix, with $L=N^2$ nonzero entries in A the radius of this circle ρ is equal to the product of the standard deviation and square root of the system size N. For nonfully connected networks, $L<N^2$, the radius is given by (see, e.g., Ref. [43])

$$\rho = \sigma_A\sqrt{L/N} = \sigma_A\sqrt{\langle k\rangle}. \tag{7}$$

If the diagonal elements of the random matrix are from a zero-mean distribution, Girko's circle is centered at the origin of the complex plane. In our case we have $A_{ii}<0$ and the center of the circle in the complex plane will be shifted to the position $(-A_{ii},0)$, see, e.g., Ref. [44,45].

A simple measure for system stability is the maximal Lyapunov exponent

$$\lambda \equiv \lim_{t\to\infty} \frac{1}{t} \ln\left(\frac{\|x(t) - x'(t)\|}{\|x(0) - x'(0)\|} \right), \tag{8}$$

where $x'(t)$ results from a small perturbation in the initial condition, $\|x(0)-x'(0)\| \ll 1$. For the system without the positivity condition λ can be related to ρ,

$$\lambda(\langle k\rangle) \sim \rho(\langle k\rangle) + A_{ii} = \sigma_A(\sqrt{\langle k\rangle} - D), \tag{9}$$

where A_{ii} is the spectrum shift discussed above.

For the full model with the positivity condition and the fixed point $x_i^0 > 0$, we hypothesize the following scenario: For $\lambda < 0$, i.e., when $\langle k\rangle$ is sufficiently small, the fixed point x^0 is stable and all trajectories x_j will be normally distributed around x^0. Suppose that the average noise amplitude per link is fixed (ξ_{ij} is an iid) then each added link will add to the noise level in the system. For iid processes with zero mean we therefore can expect the variance of the distribution of x to grow linearly with $\langle k\rangle$, i.e., $\sigma_{\delta x}^2 \propto k$, as long as $\lambda < 0$. Here $\delta x = x - x^0$ and $\sigma_{\delta x}^2 \equiv 1/N \Sigma (\delta x_j - \overline{\delta x})^2$, being the mean-square error of δx, with $\overline{\delta x} \equiv \Sigma \delta x_i / N$. Let us look at the number of nodes that are on, N_{on}, or off, N_{off}. Off nodes are those associated with the part of the distribution spread over the negative x values. For the sake of simplicity we picture the x values to be distributed around $\bar{x}^0 \equiv \Sigma_i x_i^0 / N > 0$, the mean averaged fixed point concentration. Therefore one can roughly estimate N_{on}, in the $\lambda < 0$ phase, to be proportional to one minus the integral over the part of the distribution associated with the off nodes, i.e., $N_{on}/N = [1 + \mathrm{erf}(c\bar{x}^0/\sqrt{\langle k\rangle})]/2$ for some constant c. For a better estimate one would additionally average over the distribution of x_i^0. However, we clearly get $N_{on} \to N$ as $\langle k\rangle \to 0$. On the other hand this approximation predicts $N_{on} \sim N/2$ for large $\langle k\rangle$. Since this approximation was derived for small $\langle k\rangle$, i.e., $\lambda < 0$, we need an alternative way to show that about half the nodes remain *on* for large $\langle k\rangle$, i.e., for $\lambda > 0$. For this we look at the probability $P(\dot{x}_i > 0)$ that the concentration x_i for a node i is growing. To compute it we remember that nonzero entries $|A_{ij}| > 0$ of matrix A are drawn from a Gaussian distribution and use the identity

$$\int dz_1 dz_2 \delta(w - a_1 z_1 - a_2 z_2) \frac{e^{-z_1^2/2b_1}}{\sqrt{2\pi b_1}} \frac{e^{-z_2^2/2b_2}}{\sqrt{2\pi b_2}} = \frac{e^{-w^2/2(b_1 a_1^2 + b_2 a_2^2)}}{\sqrt{2\pi(b_1 a_1^2 + b_2 a_2^2)}}, \tag{10}$$

with the equation of motion, Eq. (4), to compute

$$P(\dot{x}_i > 0) = \frac{1}{2}\mathrm{erfc}\left(\frac{D\delta x_i}{\sqrt{2\sum_{\{j:|A_{ij}|>0\}} \delta x_j^2}} \right), \tag{11}$$

with $\mathrm{erfc} \equiv 1 - \mathrm{erf}$. Approximating the expression $\Sigma_{\{j:|A_{ij}|>0\}} \delta x_j^2 \approx \langle k\rangle(\sigma_{\delta x}^2 + \overline{\delta x}^2)$, which is justified when averages and variances of δx restricted to the row-wise nonzero entries in A are sufficiently similar, we can write

$$P(\dot{x}_i > 0) \approx \frac{1}{2}\mathrm{erfc}\left(\frac{D}{\sqrt{2\langle k\rangle}} \frac{\delta x_i}{\sqrt{\sigma_{\delta x}^2 + \overline{\delta x}^2}} \right). \tag{12}$$

For large $\langle k\rangle$ this expression approaches $P(\dot{x}_i > 0) \sim 1/2$ and one can conclude that on average the fraction of decreasing or increasing concentrations both amount to one-half, $N_{on}/N \sim 1/2$.

Note that every trajectory x_i that is stopped at zero practically reduces the system size, as the dynamics of the remaining system is equivalent to deleting the ith column and row in A together with the ith entry in vector x. N_{on} is therefore a measure of the *effective* system size. Associated with N_{on} there is an effective number of links $L_{on} = LN_{on}^2/N^2$ and an effective connectivity

$$\langle k_{\mathrm{on}}\rangle = \langle k\rangle N_{\mathrm{on}}/N. \tag{13}$$

Inserting the effective connectivity into Eq. (9) gives an approximate formula for the effective Lyapunov exponent

$$\lambda \sim \sigma_A(\sqrt{\langle k_{on}\rangle} - D). \tag{14}$$

Since large $\langle k\rangle$ implies $N_{on} \sim N/2$ this leads to the high connectivity approximation

$$\lambda \sim \sigma_A\left(\sqrt{\frac{\langle k\rangle}{2}} - D \right). \tag{15}$$

These arguments show that for $\langle k\rangle < D^2$ we may expect Eq. (9) to hold while for sufficiently large $\langle k\rangle$ (we return to this point later) the Lyapunov exponent λ will start to behave like Eq. (15). This leads to *two* critical values for $\langle k\rangle$. The lower critical connectivity $\langle k\rangle_{crit}^- = D^2$ indicating the point where $\lambda = 0$ for the low-connectivity approximation, Eq. (9), and the upper critical connectivity $\langle k\rangle_{crit}^+ = 2D^2$ which is the point where $\lambda = 0$ for the high-connectivity approximation, Eq. (15).

C. Note on multiplicative noise

The diagonal component of Eq. (4) reminds of the stochastic differential equation,

$$\frac{d}{dt}x = f(x) + g(x)\xi(t) + \eta(t), \tag{16}$$

with $f = -A_{ii}x$ and $g(x) = x$. This Langevin process has been exactly solved—ignoring the positivity constraint—[41], the solution being a q-exponential, $p(x) \sim [1 + (q-1)\beta x^2]^{1/(1-q)}$, with $\beta = (-A_{ii} + \bar{\sigma}/2)/\sigma$, and $(1-q)^{-1}$ the asymptotic power exponent. In simulations we have shown that this result continues to hold when the positivity condition is taken into consideration as well. In Fig. 1(c) we show experimental data confirming the power-law aspect of mRNA levels from the yeast genome data [38,39]. Here $\Delta x_i(t) \equiv x_i(t) - x_i(t-1)$ is the difference in gene expression levels between two consecutive measurements; $P(>\Delta x)$ is the cumulative distribution, for all i and t. In the same plot we show results of a numerical simulation of the model, Eq. (4), with the $N = 6000$ ER topology for A at $\langle k\rangle = 20$, for the two cases: first, $\bar{\sigma} = 0$ and $\sigma > 0$ (Gaussian noise model), and second $\bar{\sigma} > 0$ and $\sigma = 0$ (multiplicative noise model). Data is fitted with a

q-exponential fit (broken line), with an effective $q_{\mathrm{cum}}=1.55$. (Note, the cumulative probability distribution function of a q exponential is a q exponential, with q_{cum}.)

Further note a potential stabilizing role of multiplicative noise [46]. Consider the one-dimensional case of our model,

$$\frac{d}{dt}x = a(x - x_0) + \xi x + \eta, \tag{17}$$

with $\xi \in N(0, \bar{\sigma})$ and $\eta \in N(0, \sigma)$. The evolution of a perturbation δx thus follows

$$\frac{d}{dt}\delta x = a\,\delta x + \xi \delta x, \tag{18}$$

with the solution

$$\delta x(t) = \delta x(0) e^{(a-\bar{\sigma}^2/2)t} e^{\bar{\sigma}\int dt \xi(t)}. \tag{19}$$

The Lyapunov exponent is proportional to $a - \bar{\sigma}^2/2$ showing that the system can be stable even for positive a.

III. RESULTS

We numerically solve Eq. (4) with the positivity condition Eq. (4) and compare with the above predictions. We generate SF and ER networks of sizes $N=200$, 500, 1000. To vary $\langle k \rangle$ we adjusted the number of nonzero rates L in A. For SF networks the scaling exponent was fixed to $\gamma=2.2$. All of the following results are averages over 50 random realizations of networks for a given parameter set. The Lyapunov exponents were computed from 1000 time steps, after discarding the first 200 steps. Numerical integration was done with a time increment of $dt=0.1$. x^0 was chosen from the experimental distribution of Fig. 1(b). We did not observe noteworthy changes of results when using uniform or Gaussian distributions. In Fig. 2 we show the dynamics of the model, Eq. (4), for five randomly selected trajectories, in three regions of $\langle k \rangle$, one corresponding to $\lambda < 0$ (a), one associated to critical dynamics at $\lambda = 0$ (b), and one for $\lambda > 0$ (c). In Fig. 2(a) the trajectories are in the vicinity of their fixed point x^0, and stay there even after a significant perturbation (at time $t=1000$). In Fig. 2(b) trajectories show oscillatory behavior. After perturbing with the same constant vector x^p as in (a) the trajectories continue oscillating, however, around a new steady state. Exponential divergence in the chaotic region is shown in Fig. 2(c).

In Fig. 3 the solution for λ for the ER network as a function of $\langle k \rangle$, with (triangles) and without (boxes) positivity condition, is given. The corresponding theoretical predictions, Eqs. (9) and (15), are drawn as solid and broken lines, respectively. The case without positivity condition is completely explained by theory over the entire range of $\langle k \rangle$ by Eq. (9). In the case with the constraint for small $\langle k \rangle$, Eq. (9) is valid, while the asymptote follows Eq. (15), as expected. The main finding of this paper is that within a $\langle k \rangle$ window between about $\langle k \rangle^-_{crit}$ and $\langle k \rangle^+_{crit}$ a plateau forms where λ practically vanishes (up to a precision of $|\lambda| < 0.005$).

The stability of the system for different network topologies, sizes, and various noise components is shown in Fig. 4.

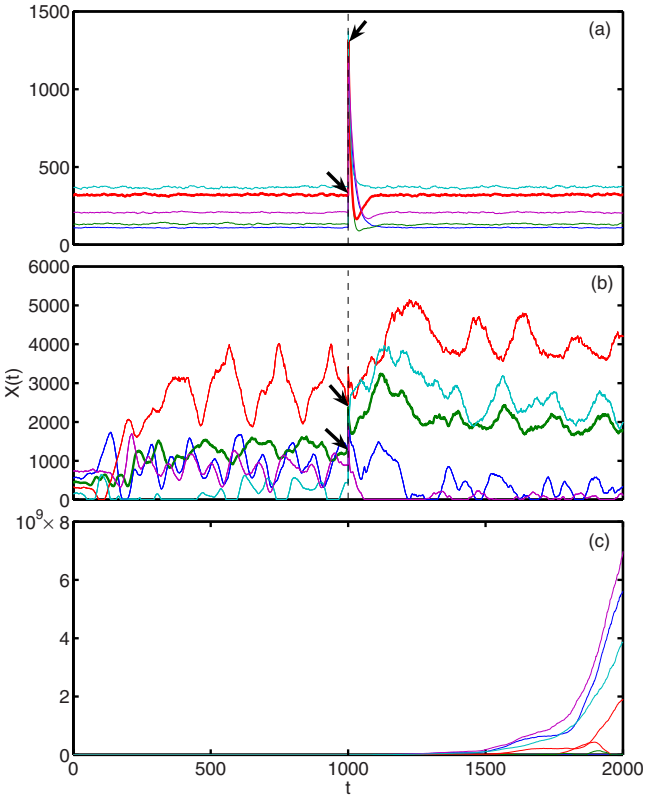

FIG. 2. (Color online) Time series of five randomly selected trajectories [numerical solutions of Eq. (4)] for the regions (a) $\lambda < 0$, (b) at the $\lambda = 0$ plateau, and (c) $\lambda > 0$. $N=500$, $\sigma=\bar{\sigma}=0.1$, and $D=4$. These trajectories have been artificially perturbed by an additive shift x^p (depicted with the arrows for one trajectory).

Figure 4(a) indicates that both network size and degree distribution are only slightly influencing the width of the plateau. While in the $\langle k \rangle \to N$ region there is no significant difference in system stability, the low connectivity region

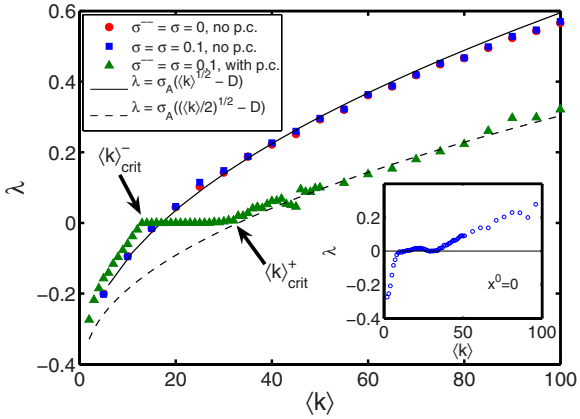

FIG. 3. (Color online) Maximum Lyapunov exponents λ as a function of average degree $\langle k \rangle$, averaged over 50 realizations for ER networks. Simulations are shown without positivity condition for noise $\sigma=\bar{\sigma}=0.1$ (squares) and without noise $\sigma=\bar{\sigma}=0$ (circles). The influence of the positivity condition on forming a plateau is demonstrated with noise $\sigma=\bar{\sigma}=0.1$ (triangles). The solid and broken lines are Eqs. (9) and (15). Inset: plateau for the case $x_j^0=0$, with noise $\sigma=\bar{\sigma}=0.1$. In all cases $N=500$, $D=4$.

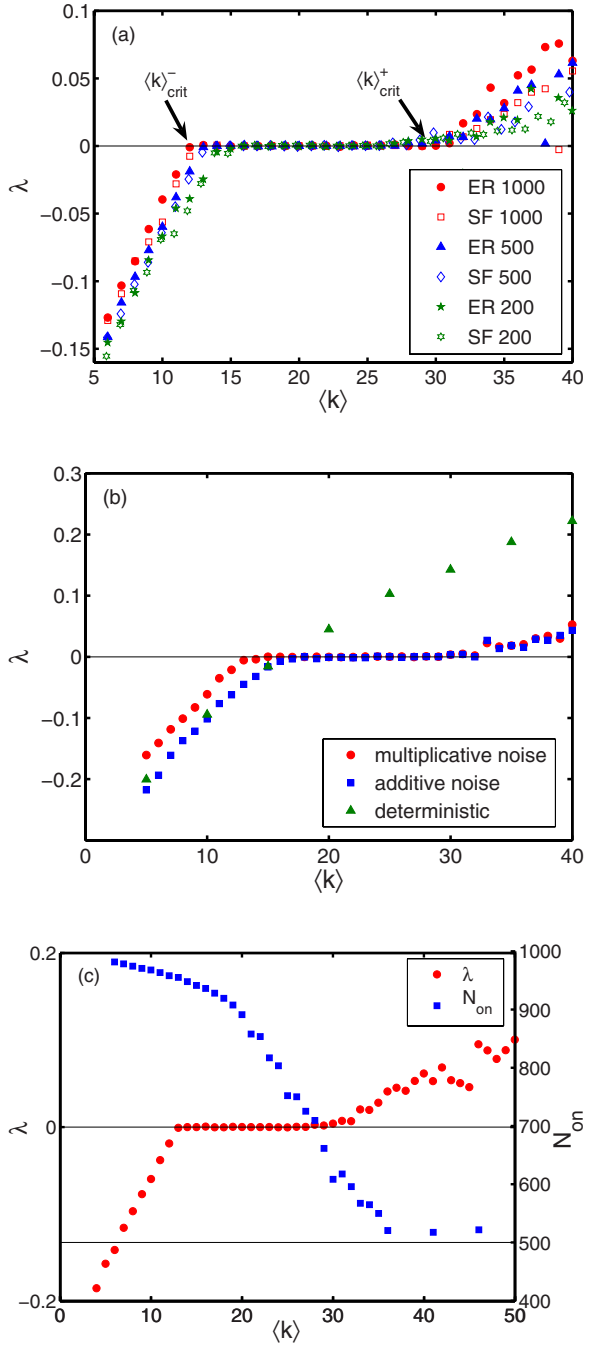

FIG. 4. (Color online) Lyapunov exponents for the same parameters as in Fig. 3 for (a) different network types and sizes $N=200$, 500, 1000, (b) noise effects for multiplicative noise ($\bar{\sigma}=0.1$ and $\sigma=0$), additive noise ($\bar{\sigma}=0$ and $\sigma=0.1$), compared to the deterministic process ($\bar{\sigma}=\sigma=0$) without the positivity condition. (c) λ compared to the number of inactive nodes as a function of connectivity. ER, $N=1000$, $D=4$, and $\sigma=\bar{\sigma}=0.1$.

shows a size effect on the $\lambda=0$ plateau. The effect of network topology is relatively small, the curve pertaining to SF always being slightly below the ER networks, see Fig. 4(a). While the width of the plateau is always wider for the random distribution of links, in the $\langle k\rangle\to 0$ region, the system is more stable (smaller λ) for SF networks. For higher connectivity regions ($\langle k\rangle \gtrsim \langle k\rangle^+_{crit}$) the difference between random and scale-free networks becomes numerically indistinguishable. Figure 4(b) shows the influence of pure multiplicative ($\bar{\sigma}>0, \sigma=0$) and pure additive noise ($\bar{\sigma}=0, \sigma>0$) on the plateau width, compared to the deterministic process, $\bar{\sigma}=\sigma=0$. With multiplicative noise the plateau widens, while additive noise hardly shows any effect (when compared to the deterministic process without the positivity condition). Plateau widths are collected in Table I. In Fig. 4(c) the number of inactive nodes is shown with λ, again as a function of $\langle k\rangle$. Finally in Fig. 5, $\lambda(\langle k\rangle)$ is shown for four values of D. The formation of the plateau appears in the interval $[D^2, 2D^2]$, i.e., between the critical connectivities $\langle k\rangle^-_{crit}$ and $\langle k\rangle^+_{crit}$.

IV. DISCUSSION

How can the formation of the plateau for the critical region at $\lambda=0$ be understood? As long as $\lambda<0$ it is only the noise that can drive concentrations x_i toward the boundary. However, the boundary will not be absorbing since the fixed point x^0 is still attractive, and the concentration has a nonzero probability to become positive again. Due to Eq. (9), for $\langle k\rangle=D^2$ the first trajectories can be expected to become unstable and are either driven toward zero or toward infinity. Trajectories that are driven toward zero are stopped there which stabilizes the system and $\lambda\sim 0$ is reattained. But what about trajectories that are driven toward infinity? Why should they be stopped? To understand this we look at $P(\Sigma_i \dot{x}_i>0)$, the probability that the sum over all concentrations is increasing. Using Eq. (10) we can derive

$$P\left(\sum_i \dot{x}_i>0\right)=\frac{1}{2}\mathrm{erfc}\left(\frac{D\sum_i \delta x_i}{\sqrt{2\sum_i \sum_{\{j:|A_{ij}|>0\}} \delta x_j^2}}\right)$$
$$\approx \frac{1}{2}\mathrm{erfc}\left(D\sqrt{\frac{N}{2\langle k\rangle}}\frac{\delta\bar{x}}{\sqrt{\sigma^2_{\delta x}+\delta\bar{x}^2}}\right), \quad (20)$$

using the same approximation as above. Due to the symmetry of the model, $\delta\bar{x}\sim 0$, as long as no trajectory has been stopped at zero. Now, since decreasing trajectories are stopped at zero this symmetry breaking causes $\delta\bar{x}>0$. Once $\delta\bar{x}>\epsilon>0$, for any constant ϵ, it follows that if N is sufficiently large compared to $\langle k\rangle$ the probability for the sum of the concentrations to grow vanishes. This indicates that with a probability of almost one the trajectories diverging to large values have to be balanced by the decreasing ones. One can therefore expect that—on average—every trajectory that is driven toward infinity by the linear dynamics requires a decreasing counterpart to do so. As a consequence, a growing trajectory gets stopped when the balancing decreasing trajectory is stopped at zero. This mechanism stabilizes the system as long as there are decreasing trajectories that *can* be stopped and thus may render a stabilizing effect. When there are no more trajectories left to be stopped, which happens

TABLE I. Zero-λ plateau widths Δ for an ER network, with $N=500$. Δ is defined as the region of connectivity where $|\lambda|<0.005$. For the situation of variable multiplicative noise the additive noise was fixed to $\sigma=0.1$, for the variable additive noise, $\bar{\sigma}=0.1$. Cases for different D are shown. For variable multiplicative noise levels the plateau grows up to a noise amplitude of $\bar{\sigma}\sim 0.1$. Very high noise levels of either kind destroy the plateau (not shown).

$D\backslash\bar{\sigma}(\sigma=0.1)$	0	0.001	0.005	0.01	0.05	0.1	0.2	0.5	0.7
2	4	3	4	5	5	5	4	2	2
4	15	16	16	17	18	19	13	12	11
6	35	36	36	37	37	36	30	20	22
$D\backslash\sigma(\bar{\sigma}=0.1)$	0	0.001	0.005	0.01	0.05	0.1	0.2	0.5	0.7
2	5	6	5	4	5	5	4	4	4
4	20	20	19	18	18	19	19	18	19
6	37	36	37	36	35	36	35	35	35

when about $N_{off}\sim N/2$ trajectories have hit zero, $\lambda\sim 0$ cannot be maintained by stopping processes. From that point on $\lambda>0$ starts to grow again as a function of $\langle k\rangle$.

In other words, the formation of the critical $\lambda=0$ plateau can be seen as a selection mechanism in which the most active reactions (largest reaction rates in A) will be directly or indirectly stopped by the boundary, which drives the system to a critical state at $\lambda=0$. The end of the plateau is characterized by the point where no trajectories are available for stopping anymore. At this point the role of parameter D becomes clear. It controls the size and the position of the plateau. The switching in the behavior of λ between Eq. (9) and Eq. (15) has the characteristics of a phase transition where $\langle k\rangle$ passes from $\langle k\rangle^{-}_{crit}=D^2$ to $\langle k\rangle^{+}_{crit}=2D^2$ while the critical parameter $\lambda=0$ remains at its critical value. These theoretical arguments allow to understand the basic mechanism of the effect of the nonlinear constraint, however, more work is needed to fully understand the precise underlying mathematical details. For example, the presented arguments rely on $x^0>0$, and numerical results indicate some deviations in the details of the formation of the plateau for the special fixed point, $x^0=0$.

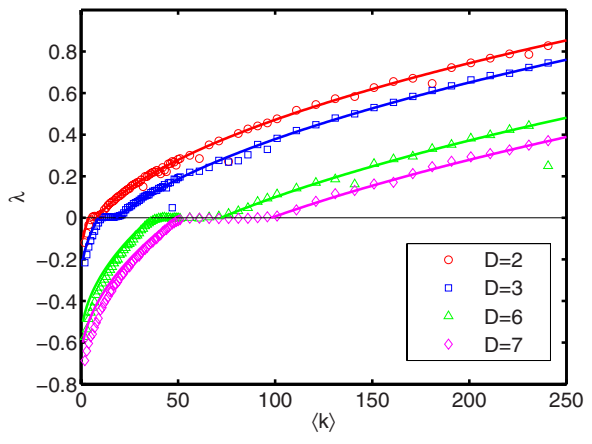

FIG. 5. (Color online) Lyapunov exponents for four different values of D. The dependence of the critical region and the width of the plateau is seen. Lines correspond to Eqs. (9) and (15).

To summarize, we have studied the stability of a simple linear model of catalytic reaction equations for cellular products such as mRNA molecules or proteins. The system is driven by intrinsic molecular noise (multiplicative) and external (additive) noise. We show that the model captures basic empirical features, such as the fat tail distribution of concentration changes. Imposing an intuitively natural constraint on the system, (non-negativity of concentrations) we observe the formation of a plateau of vanishing Lyapunov exponents in terms of the connectivities of interaction matrices. The dynamical stability of concentrations in catalytic regulatory networks, given in Eq. (4), has three extended phases in parameter space (here connectivity). In the first phase the system is asymptotically stable, λ is negative. After perturbations in this phase the system relaxes to its fixed point. The main finding of this work is the existence of a second, critical phase, where $\lambda\sim 0$ extends over a region of size D^2. This is in marked contrast to the dynamics of many other nonlinear systems, which show criticality at a singular set of points. The emergence of this phase can be fully understood within the model. At sufficiently high connectivities some products reach criticality in the linear model and those products with the largest reaction rates will—on average—start to diverge. Concentrations driven toward zero will be stopped at the boundary. Diverging concentrations are coupled with decaying concentrations and will be stopped indirectly by the boundary via stopping processes affecting their associated decaying concentrations. The stopping-process stabilizes the system at criticality as long as there are potentially decaying concentrations left to be stopped at zero. In the third phase, defined by $\lambda>0$, the system is dynamically unstable and concentration levels are diverging. The existence of these three phases corresponds perfectly with the observation made in Refs. [17,24] that these three phases might be universal for a wide class of recurrent networks.

Technically, we discussed the dependence of the $\lambda=0$ plateau on two network topologies, ER and SF. A remarkably small influence of the topology on the plateau was found. We found that multiplicative noise influences the size of the plateau while additive noise shows practically no effect.

In Ref. [47] it was noted that neural networks can perform most complex computations if the dynamics of random

threshold gate networks is at the critical boundary between the ordered and chaotic regime. If we interpret gene-regulatory networks as computing devices performing hundreds of optimization problems simultaneously, it is plausible that evolution would have selected among the most efficient variations—working at the edge of chaos.

ACKNOWLEDGMENTS

Supported by WWTF Life Science Grant No. LS 139, and by Austrian Science Fund FWF, Project No. P19132. The present model was designed by R.H. and S.T., numerical work was done by D.S., the paper was written by S.T.

[1] C. Langton, Physica D **42**, 12 (1990).
[2] S. Kauffman, *The Origins of Order: Self-Organization and Selection in Evolution* (Oxford University Press, New York, 1993).
[3] M. Mitchell, P. Hraber, and J. Crutchfield, Complex Syst. **7**, 89 (1993).
[4] N. Packard, *Dynamic Patterns in Complex Systems* (World Scientific, Singapore, 1988), pp. 293–301.
[5] P. Melby, J. Kaidel, N. Weber, and A. Hübler, Phys. Rev. Lett. **84**, 5991 (2000).
[6] A. Robledo, Europhys. News **36**, 214 (2005).
[7] M. Eigen, Naturwissenschaften **58**, 465 (1971).
[8] A. Lotka, J. Phys. Chem. **14**, 271 (1910).
[9] A. Pross and V. Khodorkovsky, J. Phys. Org. Chem. **17**, 312 (2004).
[10] A. Pross, Pure Appl. Chem. **77**, 1905 (2005).
[11] S. Maslov and K. Sneppen, Science **296**, 910 (2002).
[12] H. Jeong, S. Mason, A.-L. Barabási, and Z. Oltvai, Nature (London) **411**, 41 (2001).
[13] H. Jeong, B. Tombor, B. Albert, Z. Oltvai, and A.-L. Barabási, Nature (London) **407**, 651 (2000).
[14] D. Wolf and F. Eeckman, J. Theor. Biol. **195**, 167 (1998).
[15] N. Holter, A. Maritan, M. Cieplak, N. Fedoroff, and J. Banavar, Proc. Natl. Acad. Sci. U.S.A. **98**, 1693 (2001).
[16] S. Kikuchi, D. Tominaga, M. Arita, K. Takahashi, and M. Tomita, Bioinformatics **19**, 643 (2003).
[17] L. Glass and S. Kauffman, J. Theor. Biol. **39**, 103 (1973).
[18] H. Smith, J. Math. Biol. **25**, 169 (1987).
[19] J. Mahaffy, D. Jorgensen, and R. van der Heyden, J. Math. Biol. **30**, 669 (1992).
[20] T. Mestl, C. Lemay, and L. Glass, Physica D **98**, 33 (1996).
[21] T. Chen, H. He, and G. Church, Pac. Symp. Biocomput 29 (1999).
[22] H. McAdams and L. Shapiro, Science **269**, 650 (1995).
[23] R. Yoshida, S. Imoto, and T. Higuchi, *Proceedings IEEE 4th Computational Systems Bioinformatics* (IEEE, Los Alamitos, CA, 2005), pp. 289–298.
[24] M. Andrecut and S. Kauffman, New J. Phys. **8**, 148 (2006).
[25] M. Ko, Bioessays **14**, 341 (1992).
[26] S. Fiering, E. Whitelaw, and D. Martin, Bioessays **22**, 381 (2000).
[27] J. Hasty, J. Pradines, M. Dolnik, and J. Collins, Proc. Natl. Acad. Sci. U.S.A. **97**, 2075 (2000).
[28] P. Heitzler and P. Simpson, Cell **64**, 1083 (1991).
[29] P. Guptasarma, Bioessays **17**, 987 (1995).
[30] M. Elowitz, A. Levine, E. Siggia, and P. Swain, Science **297**, 1183 (2002).
[31] K.-C. Chen, T.-Y. Wang, H.-H. Tseng, C.-Y. Huang, and C.-Y. Kao, Bioinformatics **21**, 2883 (2005).
[32] L. Michaelis and M. Menten, Biochem. Z. **49**, 333 (1913).
[33] J. Hofbauer and K. Sigmund, *Evolutionary Games and Population Dynamics* (Cambridge University Press, Cambridge, England, 1998).
[34] S. Jain and S. Krishna, Phys. Rev. Lett. **81**, 5684 (1998).
[35] S. Jain and S. Krishna, Proc. Natl. Acad. Sci. U.S.A. **99**, 2055 (2002).
[36] M. Yeung, J. Tegner, and J. Collins, Proc. Natl. Acad. Sci. U.S.A. **99**, 6163 (2002).
[37] P. D'Haeseler, X. Wen, S. Fuhrman, and R. Somogoyi, Pac. Symp. Biocomput **4**, 41 (1999).
[38] R. Cho *et al.*, Mol. Cell **2**, 65 (1998).
[39] J. Zivkovic, B. Tadic, N. Wick, and S. Thurner, Eur. Phys. J. B **50**, 255 (2006).
[40] P. Erdös and A. Rényi, Publ. Math. (Debrecen) **6**, 290 (1959).
[41] C. Anteneodo and C. Tsallis, J. Math. Phys. **44**, 5194 (2003).
[42] V. Girko, Theory Probab. Appl. **29**, 694 (1985).
[43] A. Crisanti, G. Paladin, and A. Vulpiani, *Products of Random Matrices* (Springer-Verlag, Berlin, 1993).
[44] C. Biely and S. Thurner, Quant. Finance (in press).
[45] S. Thurner and C. Biely, Acta Physiol. Pol. **38**, 4111 (2007).
[46] R. Khas'minskii, Theory Probab. Appl. **12**, 144 (1967).
[47] N. Bertschinger and T. Natschläger, Neural Comput. **16**, 1413 (2004).